

Determination of Geostationary Orbits (GEO) Satellite Orbits Using Optical Wide-Field Patrol Network (OWL-Net) Data

Bumjoon Shin, Eunji Lee, Sang-Young Park[†]

Department of Astronomy, Yonsei University, Seoul 03722, Korea

In this study, a batch least square estimator that utilizes optical observation data is developed and utilized to determine geostationary orbits (GEO). Through numerical simulations, the effects of error sources, such as clock errors, measurement noise, and the a priori state error, are analyzed. The actual optical tracking data of a GEO satellite, the Communication, Ocean and Meteorological Satellite (COMS), provided by the optical wide-field patrol network (OWL-Net) is used with the developed batch filter for orbit determination. The accuracy of the determined orbit is evaluated by comparison with two-line elements (TLE) and confirmed as proper for the continuous monitoring of GEO objects. Also, the measurement residuals are converged to several arcseconds, corresponding to the OWL-Net performance. Based on these analyses, it is verified that the independent operation of electro-optic space surveillance systems is possible, and the ephemerides of space objects can be obtained.

Keywords: electro-optical surveillance system, optical wide-field patrol network (OWL-Net), batch filter, orbit determination, geostationary satellite, Communication, Ocean and Meteorological Satellite (COMS)

1. INTRODUCTION

Space surveillance systems, based on electro-optic systems, have been mainly developed in advanced countries since the early 1990s due to the increased risk posed by space objects. An electro-optic space surveillance system takes a visible image of a space object using the sunlight reflected from that object to determine its size and direction; this procedure is similar to making astronomical observations. As these systems use the light reflected from the space object, it is applicable to objects in low earth orbit (LEO), geostationary orbit (GEO), and even heliocentric orbit. Recently, studies on electro-optic space surveillance systems have been conducted, including studies on the tracking of GEO satellites (Vallado et al. 2010), and the determination of various types of information such as the location, velocity, mass distribution, rotational ratio, and attitude of space objects based on photometric and space geodesy data obtained through optical observations (Linares et al. 2013).

The optical wide-field patrol network (OWL-Net) is the first Korean optical surveillance system of space objects, constructed to protect space assets by tracking and monitoring domestic satellites. The system was developed by the Korea Astronomy and Space Science Institute (KASI), and makes use of five observatories in Korea, Mongolia, Morocco, Israel, and the USA. Measurement data composed of topocentric right ascension and declination is extracted from the image pixel coordinates (Park et al. 2013). The observation data from OWL-Net is validated with the quality of a few arcseconds, and the orbit solutions for LEO satellites with the accuracy of tens of meters are obtained by using a batch estimator with the OWL-Net data (Choi et al. 2018). Also, the observation data for a domestic GEO satellite obtained by OWL-Net was analyzed and employed to achieve orbit solutions using orbit determination toolkit (ODTK), a commercial software package, and the accuracy was about 2 km (Son 2015).

In this study, orbit determination (OD) software employing a batch filter is developed to independently

© This is an Open Access article distributed under the terms of the Creative Commons Attribution Non-Commercial License (<https://creativecommons.org/licenses/by-nc/3.0/>) which permits unrestricted non-commercial use, distribution, and reproduction in any medium, provided the original work is properly cited.

Received 13 JUN 2019 Revised 14 AUG 2019 Accepted 25 AUG 2019

[†]Corresponding Author

Tel: +82-2-2123-5687, E-mail: spark624@yonsei.ac.kr

ORCID: <https://orcid.org/0000-0002-1962-4038>

operate a space surveillance system. Moreover, this software generates pseudo-optical observation data to examine the effects of the arc length, observation intervals, clock errors, noise, and a priori uncertainty on the accuracy of the OD for a GEO satellite. It is significant that the optical observation data for a domestic geostationary satellite taken from OWL-Net is analyzed using the developed software. This technology facilitates the independent management of orbit information derived from the Korean space surveillance system.

In Chapter 2, the methodology used for the development and verification of the OD algorithm are described. In Chapter 3, the properties of the OD for the GEO satellite are analyzed using pseudo-optical observation data generated in the same form as OWL-Net data with various properties such as the arc length and intervals, clock errors, noise, and a priori uncertainty. In Chapter 4, practical optical observation data of Communication, Ocean and Meteorological Satellite (COMS) is applied to the developed software and the orbit solution is analyzed by comparing to two-line elements (TLE). In Chapter 5, the research results and significance are presented.

2. BATCH LEAST SQUARES FILTER AND VERIFICATION

2.1 Methodology

Although sequential estimation is better suited to real-time monitoring compared to a batch-type estimator, the batch-type estimator is more accurate and robust (Crassidis & Junkins 2011). Considering the objective of this study, to obtain accurate orbit solution for long-time prediction, and the process of the optical tracking system where the measurement data is extracted from optical images after observations, the batch least squares method was employed in this work. The batch least squares is the simplest method of estimating epoch states using a set of observed data over a period. Fig. 1 shows a flowchart of the batch least squares filter process, and the notation used in the figure is equivalent to the following description.

A batch filter algorithm estimates a value that can be used to minimize a residual between a value predicted by a system model (F) and a practical observation data set (Y) which consists of N data points, as shown in Eq. (1).

$$Y = F(X,Z) + \varepsilon \tag{1}$$

On the right side, X is the solve-for vector, Z is the

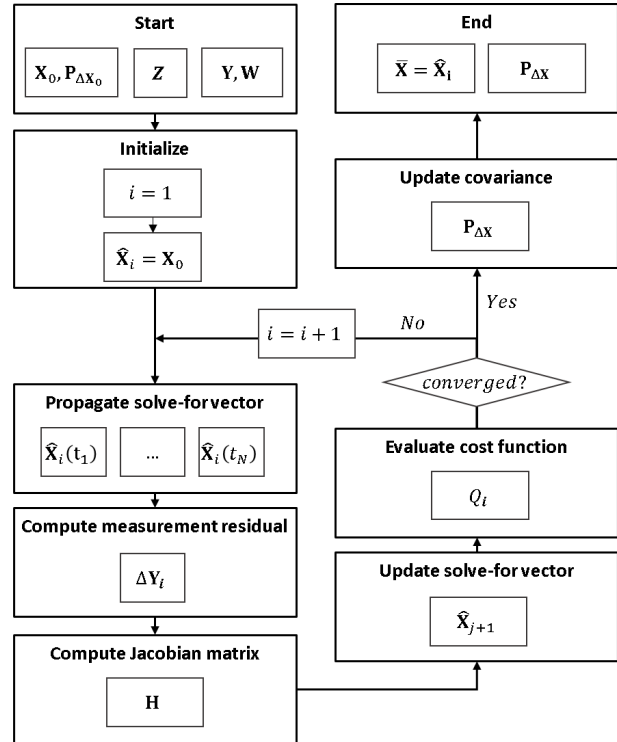


Fig. 1. Flowchart of the batch least squares estimator.

considered vector, and ϵ is the observation error. The solve-for vector has a specific uncertainty, reflected in the form of the covariance matrix. This estimation method can be described as an optimization problem used to find a solution that can minimize an objective function (Q), as shown in Eq. (2) (Schutz et al. 2004).

$$Q(X) = [Y - F(X,Z)]^T W [Y - F(X,Z)] + [X - X_0]^T [P_{\Delta X_0}]^{-1} [X - X_0] \tag{2}$$

where W is a weight matrix that consists of the inverse of the variance of each observation, and X_0 and $P_{\Delta X_0}$ are the a priori solve-for vector and covariance matrix, respectively.

Under the assumption that the solve-for vector of the i^{th} iteration (\hat{X}_i) is sufficiently close to the optimal solution (\bar{X}), the above system and objective function can be linearized based on a Taylor series, and the solve-for vector is then updated by solving a normal equation as Eq. (3). Note that the considered vector is excluded from the linearization process as it is not an estimation target (Long et al. 1989).

$$\Delta \hat{X}_i = (H^T W H + P_{\Delta X_0}^{-1})^{-1} (H^T W \Delta Y_i + P_{\Delta X_0}^{-1} (\hat{X}_{i-1} - X_0))$$

$$\hat{X}_i = \hat{X}_{i-1} + \Delta \hat{X}_i \tag{3}$$

where ΔY_i is the measurement residual of the i^{th} iteration derived as Eq. (4).

$$\Delta Y_i = [Y_1 - F(\hat{X}_i(t_1), Z) \dots Y_N - F(\hat{X}_i(t_N), Z)]^T \quad (4)$$

H is the Jacobian matrix, a partial differential equation of the system model with respect to the solve-for vector. In the OD problem, the system model is composed of a dynamics model and an observation model, and the Jacobian matrix can be expressed by the multiplication of a state transition matrix (Φ) and a sensitivity matrix (A) based on the chain rule (Long et al. 1989).

$$H = A\Phi \quad (5)$$

This iterative process is repeated until the cost reduction ratio is smaller than the criteria (ε), as in Eq. (6).

$$\frac{Q_i - Q_{i-1}}{Q_i} < \varepsilon \quad (6)$$

A covariance matrix which indicates the accuracy of the estimation result is shown in Eq. (7).

$$P_{\Delta X} = (H^T W H + P_{\Delta X_0}^{-1})^{-1} \quad (7)$$

In this study, the batch estimator was developed in the Matlab environment employing the General Mission Analysis Tool (GMAT) as the dynamics model. GMAT was developed and released for public use by NASA, and the force models and numerical integrator in the software have been verified and applied to practical mission analysis (Hughes et al. 2014).

2.2 Software Verification

A covariance matrix calculated through a batch filter indicates the accuracy of the derived estimation results based on a system model and the observation quality. The statistical validity of the algorithm can be verified by confirming the consistency between the covariance matrix and practical OD estimation results from a Monte Carlo simulation. The Monte Carlo simulation was conducted 1,000 times using a priori state error corresponding to the a priori covariance and pseudo-observations with Gaussian errors reflecting observation noise. The verification was conducted for GEO, similar to previous research where the same process was used for LEO (Lee et al. 2017). The details of the simulation environment used to verify the batch filter are described in Table 1. The reference orbit was defined in the form of Keplerian orbit elements, and the force model was set as two-body motion for simplicity. A single observatory located in Daedeok was employed, and several properties were specified for generating pseudo-observations: path length is the total time-span required to take optical images, exposure time is the time-span of an image, exposure period is the period between successive images, data frequency is the frequency used to extract data points from the image, and noise is a standard deviation of white noise. Fig. 2 shows a comparison of the estimation errors of the Monte Carlo simulation and covariance ellipsoid. The results of the Monte Carlo simulation show that 99% of the OD estimation results fall within a 3σ error range estimated by the covariance ellipsoid. This verifies that the estimation is statistically reliable and that the covariance matrix can be used to analyze the accuracy of the results.

Table 1. Simulation environment for verification of batch least squares algorithm

	Property	Value
Orbit	Epoch time (UTC)	01 Jan 2015 11:22:34
	Semi-major axis (km)	42,165.706
	Eccentricity	2.7417e-4
	Inclination (°)	0.046
	Right ascension of ascending node (°)	52.2379
	Argument of perigee (°)	249.3743
	True anomaly (°)	108.8982
Dynamic model	Force model	2-body
	Propagator	Runge-Kutta (8th order)
Estimation	Convergence criteria	$\Delta RMS / RMS < 10^{-3}$
A priori uncertainty	Position (km)	10
	Velocity (km/s)	0.01
Measurement	Path length (sec)	72,000
	Exposure time (sec)	4
	Exposure period (sec)	20
	Data frequency (Hz)	10
	Noise (arcsec)	1

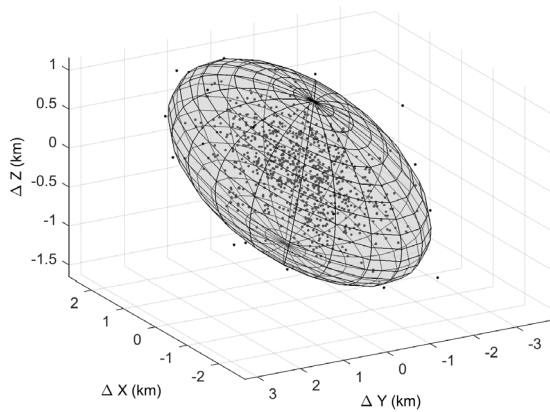


Fig. 2. Position error of Monte Carlo simulation and covariance ellipsoid.

3. CHARACTERISTICS ANALYSIS OF OD RESULTS

In this section, the accuracies of the OD results are examined by numerical simulations according to the arc length, observation interval, clock error, noise, and a priori uncertainty. The pseudo-observation data of the GEO satellite used for the analysis was generated employing an observatory in Daedeok. The target orbital elements, dynamics model, and estimation options applied to the batch filter are indicated in Table 2. The OD accuracy was evaluated by comparing the estimated states to the reference states.

3.1 Effect of Arc Length on OD Accuracy

In this section, the effect of the arc length, i.e., the time of a path of the observation, on the OD accuracy is analyzed. In general, the arc length of an object in GEO is about hours while that of an object in LEO is about 5 minutes.

In the numerical simulation, the arc length was gradually increased to 72,000 seconds (20 hours), while the other conditions such as the observation interval were maintained at constant values. Fig. 3 shows a comparison of the position and velocity errors according to the arc length when the level of noise was 1 and 100 arcseconds. For the observation data with 100 arcseconds of noise, for instance, the position errors were 89 km when the arc length was 7,200 seconds (2 hours) and 0.5 km when the arc length was 72,000 seconds (20 hours). This shows that the accuracy of the OD with low-quality (high-level noise) observation data improves significantly as the arc length increases.

The detailed trends of the accuracy of the estimation according to the arc length with a realistic noise level, under 20 arcseconds, are described in Fig. 4. The result shows that the accuracy of the OD significantly improves as the arc length increases; when the arc length was 10 times longer, the accuracy of the position and velocity improved by a

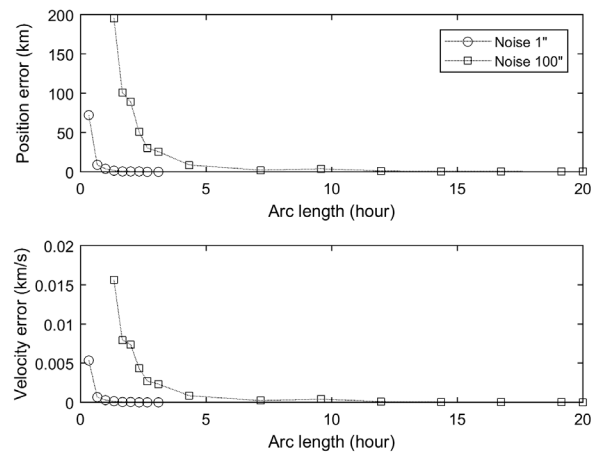


Fig. 3. Correlation of orbit determination accuracy with respect to arc length with large noise.

Table 2. Simulation environments for all kinds of error analysis

	Property	Value
Orbit	Epoch time (UTC)	01 Jan 2015 11:22:34
	Semi-major axis (km)	42,165.706
	Eccentricity	2.7417e-4
	Inclination (°)	0.046
	Right ascension of ascending node (°)	52.2379
	Argument of perigee (°)	249.3743
	True anomaly (°)	108.8982
Dynamic model	Force model	EGM96 40 × 40 3 rd body effect of all planets Solar radiation pressure Air drag (Jacchia-roboterts)
	Propagator	Runge-Kutta (8th order)
	Solve-for parameter	Position and velocity (J2000)
Estimation	Convergence criteria	$\Delta RMS / RMS < 10^{-3}$

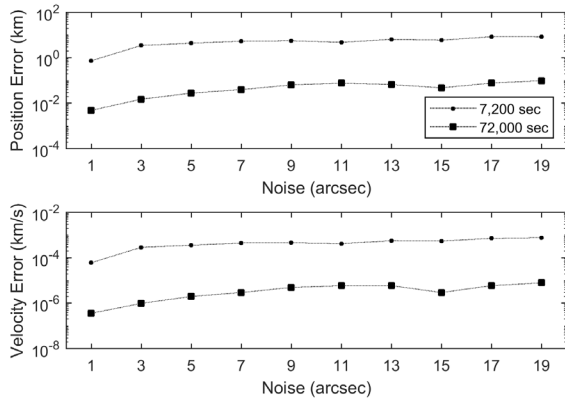


Fig. 4. Correlation of orbit determination accuracy with respect to noise level, with arc length of 7,200 and 72,000 seconds (log scale).

factor of 100 or higher. For example, the position error was 5 km when the level of noise was 5 arc-seconds and the arc length was 7,200 seconds, and that error became 20 m when the level of noise was same but arc length was increased to 72,000 seconds.

This improvement can be mathematically explained by the number of observation data points. It is clear that the first term in Eq. (7) can be expressed as the summation of each Jacobian if the weight matrix is diagonal, i.e., each observation data point is independent, as shown in Eq. (8). Since the entry of the term is applied to an inverse of the covariance, increasing the number of observation data points improves the accuracy.

$$H^T W H = \sum_{i=1}^N H_i^T W_i H_i \quad (8)$$

The accuracy of the OD was examined under conditions with a consistent number of observation data points and an increasing arc length from 250 to 10,000 seconds. Contrary to the previous analysis, the number of observation data points was maintained in the range of 1,700–1,790 by adjusting the observation interval as the arc length was varied. Using a consistent number of observations, the position errors were on the order of hundreds of kilometers and hundreds of meters for arc lengths of 250 and 10,000 seconds, respectively, and the velocity errors were 2.18 and 0.04 m/s for these arc lengths (Fig. 5). This shows that the accuracy of OD tends to improve with increase in the observation arc length, which occurs because more dynamical information about the orbit is provided by a longer time of observation.

3.2 Effect of Observation Interval on OD Accuracy

The accuracy of the OD for the GEO satellite was analyzed

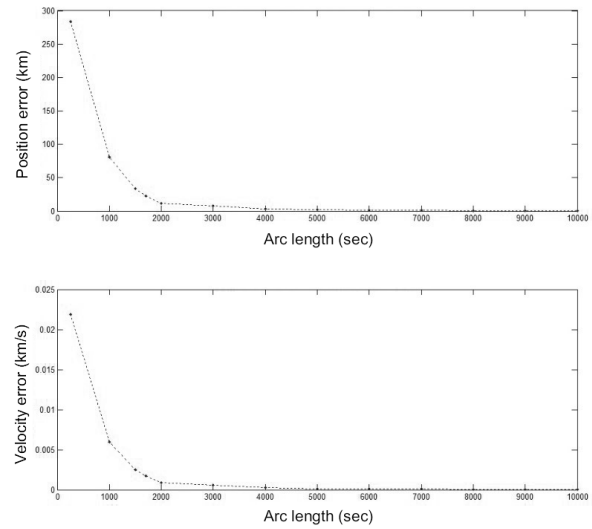


Fig. 5. Correlation of orbit determination accuracy with respect to arc length with a fixed number of observation data points.

using various observation intervals, with the condition of a fixed arc length of 7,200 seconds and a noise level varying from 1 to 20 arcseconds. The accuracy of the OD tends to increase as the observation interval is shortened (Fig. 6). As shown in Fig. 6, the sensitivity to the interval increases as the level of noise increases: the difference between the position errors at the observational intervals of 60 and 300 seconds were 2.1 km and 19 km when the noise levels were 5 and 20 arcseconds, respectively.

It was found that the observation interval does not significantly affect the OD accuracy, especially with high-quality (low-level noise) observation data. Compared to

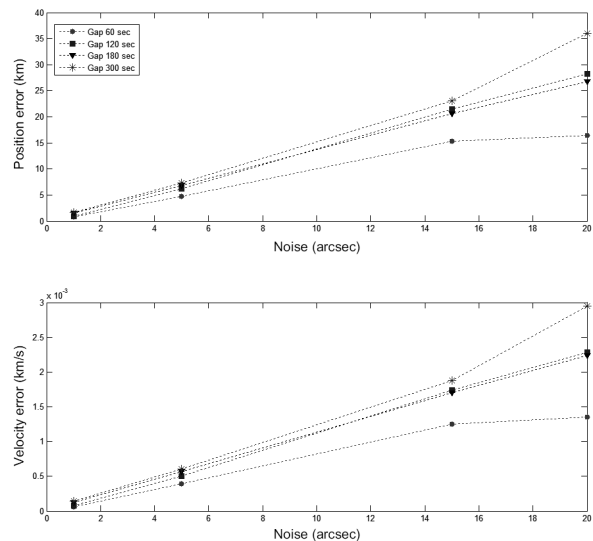


Fig. 6. Correlation of orbit determination accuracy with respect to observation interval.

the results presented in Section 3.1, the arc length is more significant than the observation interval, which indicates that it is more effective for precise OD to adjust the arc length, not the observation interval.

3.3 Effect of a Priori Uncertainty on OD Accuracy

The a priori value of the solve-for vector is not clearly identified and has a specific uncertainty reflected in the form of an a priori covariance matrix. In this section, the effects of the a priori uncertainty on the accuracy of the OD are analyzed for the LEO and GEO cases. Fig. 7 shows the positional accuracy of the OD with respect to the a priori position uncertainty for LEO and GEO satellites with a noise level of 20 arcseconds. It indicates that the positional accuracy for LEO is within 200 m regardless of the a priori uncertainty, while that of the GEO satellite tends to increase as the a priori uncertainty increases. This result can be mathematically interpreted using the sensitivity matrix, which represents the relation between the solve-for vector and the observation. A large value of the matrix indicates that the solve-for vector can significantly change the measurement data. In the case of the angles-only measurement, the sensitivity matrix of a GEO satellite with a high altitude has small values while that of an LEO satellite is large, and it is geometrically comprehensible. This can be also explained mathematically. According to the definition of the final covariance (Eq. 6), the smaller sensitivity matrix exerts less influence on the final covariance and the effect of the a priori covariance is relatively large. Practically, the a priori covariance has more of an effect on the estimation precision in the GEO case than the LEO.

To verify this mathematical analysis, the OD results for the GEO satellite are compared using two cases: case 1 excludes the a priori covariance from the objective function and the normal equation, while case 2 employs the original components (Eq. 2, Eq. 3). The OD was carried out under the conditions of a priori uncertainty varying from 10 km to 300

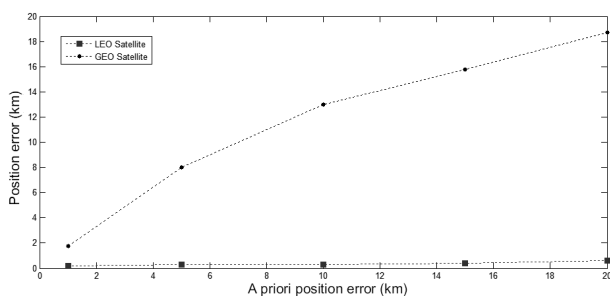


Fig. 7. Correlation of OD accuracy with respect to a priori uncertainty for LEO and GEO satellites. OD, orbit determination; LEO, low earth orbit; GEO, geostationary orbits.

km for the position, 0.01 km/s to 0.3 km/s for the velocity, and a level of noise from 1 to 500 arcseconds. The upper and lower figures in Fig. 8 show the positional accuracy of case 1 and case 2, respectively. In both cases, the effect of the a priori covariance matrix is insignificant with the low noise level. With the high noise level, however, the OD error is always within the a priori uncertainty in case 2, while in case 1, it increases without limit and proportionally to the level of noise, regardless of the a priori error. This indicates that the a priori covariance matrix prevents divergence or significant error compared to the measurement error.

Each effect of the a priori covariance and a priori error was separately analyzed using another two cases: case 3 employs a fixed a priori error and varying a priori covariance, and case 4 takes a fixed a priori covariance and changing a priori error. Each case is divided into two sub-cases based on position and velocity. Case 3-1 includes fixed a priori error of 50 km and 0.05 km/s, while case 3-2 includes fixed a priori errors of 150 km and 0.15 km/s. A fixed a priori covariance matrix of 100 km and 0.1 km/s was used for case 4-1, and 150 km and 0.15 km/s for case 4-2. Note that the noise level was set from 10 to 400 arcseconds for all cases to check the trends, even though it is much larger than the actual value.

Fig. 9 exhibits the position error of case 3, which is within tens of kilometers with the covariance of under 100 km, even though the noise increases. A position error of larger than hundreds of kilometers was found when the covariance matrix implied 1,000 km in both sub-cases, and the dependence on the noise increased as the a priori error was increased. Fig. 10 presents the positional accuracy of case 4. It shows that the accuracy is independent of the a priori error when the noise level is 10 arcseconds, i.e., the OD is robust to a priori error with high-quality

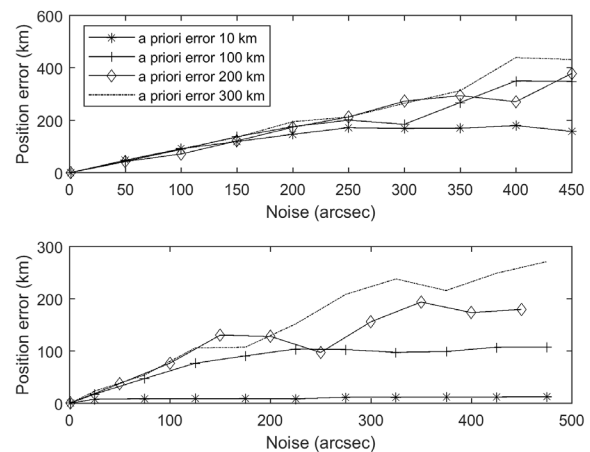


Fig. 8. Positional accuracy without the a priori covariance matrix (upper) and with the matrix (lower).

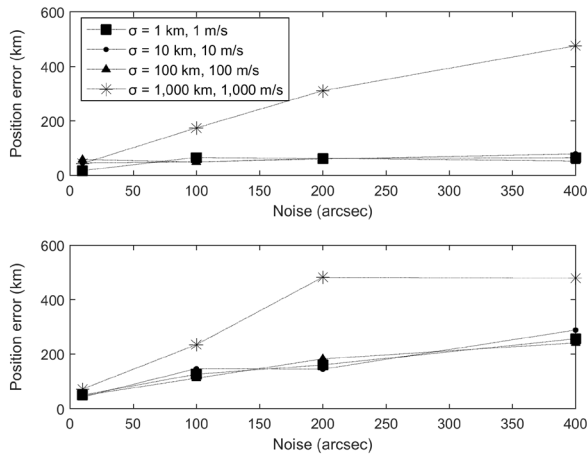


Fig. 9. Positional accuracy according to the a priori covariance matrix with fixed a priori error of 50 km and 50 m/s (upper: case 3-1) and 150 km and 150 m/s (lower: case 3-2) in position and velocity.

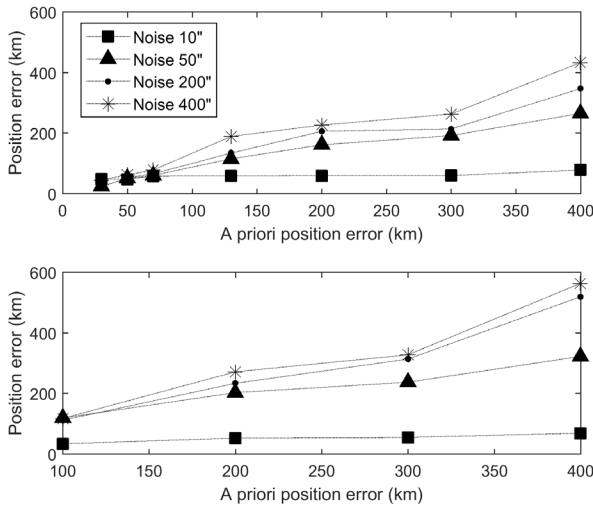


Fig. 10. Positional accuracy according to the a priori error with fixed a priori covariance of 100 km and 100 m/s (upper: case 4-1) and 150 km and 150 m/s (lower: case 4-2) in position and velocity.

measurement data. Furthermore, the OD error is within the a priori covariance ellipsoid centered at the a priori error in all sub-cases. This verifies that the a priori covariance matrix prevents a significant scatter of the estimated states from the a priori states. In other words, the estimation accuracy is determined by the noise level if the a priori covariance covers the actual error. If not, the estimated states would be near the a priori states and the accuracy is depressed.

Through these analyses, it is confirmed that the a priori covariance is significant in the OD for GEO, especially when the measurement quality is poor. Therefore, an appropriate a priori covariance matrix based on the actual reliability of the a priori state vector must be applied to obtain more accurate OD results. The robustness of the OD with respect

to the a priori error is also proved, i.e., the orbit solution can be obtained with an uncertain a priori state with a position error of 400 km.

3.4 Effect of Measurement Noise on OD Accuracy

In this section, Monte Carlo simulation with varying noise levels was carried out to analyze the effects of observation noise on the OD accuracy. Note that the noise was set from 1 to 100 arcseconds, unlike the actual value of several arcseconds, for characteristics analysis. Fig. 11 describes the changes in the accuracy of position and velocity according to the noise level, with fixed a priori errors of 10 km and 1 m/s in position and velocity. Just as in the analysis of an LEO satellite (Lee et al. 2017), the OD error in the GEO case also increases as the noise level of noise increases. The position error ranged from 0.4 to 30 km, and the velocity error reached from 0.1 to 1 m/s.

Geometrically, the angular distances corresponding to 5 and 100 arcseconds are 0.01 and 0.33 km at an altitude of 700 km (LEO) and 0.86 and 17.34 km at an altitude of 35,790 km (GEO), respectively. This analysis is consistent with the above results, where the accuracy of the OD decreases as the noise increases. The magnitude of the error in Fig. 11, however, is larger than the geometric analysis because the analysis only considers the projected position error without the line-of-sight error.

3.5 Effect of Clock Error on OD Accuracy

When extracting data from OWL-Net, two processes are performed: one process synchronizes the observation data and time, and the other combines the time log from the time

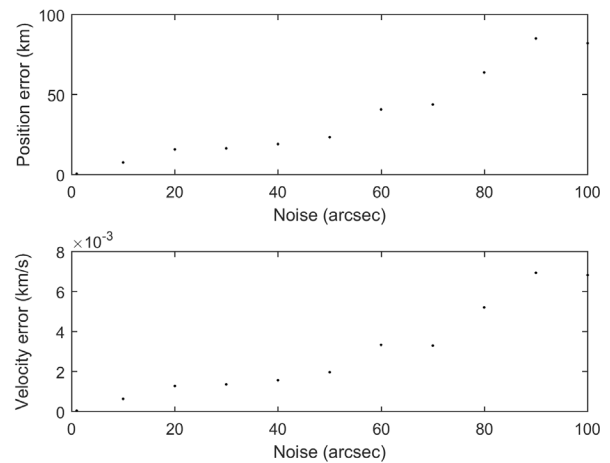


Fig. 11. Correlation of orbit determination accuracy with respect to the measurement noise.

server and extracted observation data (Park et al. 2018). Clock errors can occur in the second process, and the OD accuracy for GEO was analyzed by considering two cases: case 5 deals with a clock offset, i.e., an identical clock error is applied to the entire set of observation data, while case 6 handles a clock mismatch, i.e., a clock error is partially applied to the observation data. Case 6 is divided into sub-cases 6-1, 6-2, and 6-3, corresponding to clock mismatches on 25%, 50%, and 75% of the total observation data in each case. The level of observation noise was fixed as 15 arcseconds, and each case was repeated 100 times to obtain statistical results.

Fig. 12 shows the results of GEO OD according to the clock error. In case 5, the position error was about 3 km, which corresponds to the orbital motion of the GEO satellite, 3 km/s. On the other hand, in case 6, the accuracy was worse than that in case 5 because the clock mismatch serves as a non-linear error in the observation data which considerably degrades the OD accuracy. These results indicate that clock mismatch can cause significant estimation error, so such

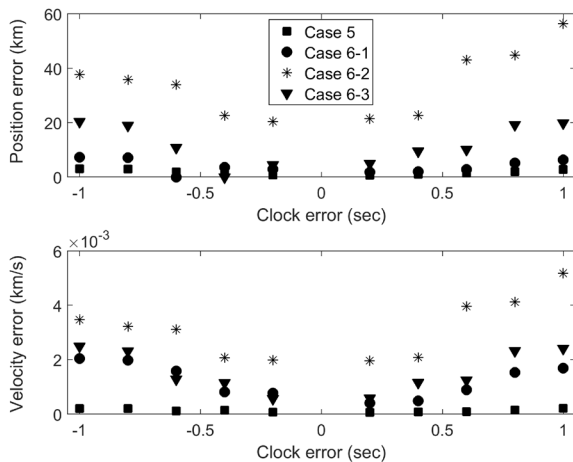


Fig. 12. Orbit determination accuracy respect to the clock errors (case 5: clock offset, case 6: clock mismatch).

errors should be corrected for accurate OD results.

4. APPLICATION OF ACTUAL DATA FROM OWL-NET

The OWL-Net data of COMS observed from Daedeok observatory was applied to the developed software. The orbit was determined and the accuracy was evaluated by comparing to TLE, whose accuracy is analyzed in Section 4.1. Moreover, the results of the error analysis in Section 3 and the practical availability were analyzed with the actual data. A fundamental dynamics model and filtering conditions for using the practical observation data are indicated in Table 3. Note that some errors such as the light travel time and annual and diurnal aberration were corrected before the analysis.

4.1 TLE Analysis for COMS

Since TLE is employed as the reference orbit, the accuracy of TLE was evaluated by an overlap analysis, prior to the OD. For the overlap analysis, successive TLEs are propagated for a certain time to generate an overlap period, and the difference between two trajectories are compared for that period. The overlap analysis was conducted for TLEs of COMS over a month, and Fig. 13 shows the results in the form of the position and velocity. The position error is on the order of tens of kilometers, which corresponds to about 0.1 degrees of angular error at an altitude of 35,790 km and is similar to the position error in the TLE information (Tombasco et al. 2011).

TLE is also assessed by the measurement residual from the actual tracking of COMS from OWL-Net (Fig. 14). The typical residual values are tens of arcseconds, excepting the irregular jump to 0.1 degrees at about four hours after the observations started. The residuals correspond to a position error of several kilometers, which coincides with the overlap

Table 3. Configuration of the OD for COMS using OWL-Net data

Property		Value
Dynamic model	Force model	EGM96 40 × 40
		3 rd body effect of all planets
		Solar radiation pressure
	Air drag (Jacchia-Roberts)	
	Propagator	Runge-Kutta (8th order)
	Method	Propagated TLE
A priori states	Uncertainty (1σ)	10 km (position) 10 m/s (velocity)
	Solve-for parameter	Position and velocity (J2000)
Estimation	Convergence criteria	ΔRMS / RMS < 10 ⁻³

OD, orbit determination; COMS, Communication, Ocean and Meteorological Satellite; OWL-Net, optical wide-field patrol network; TLE, two-line elements.

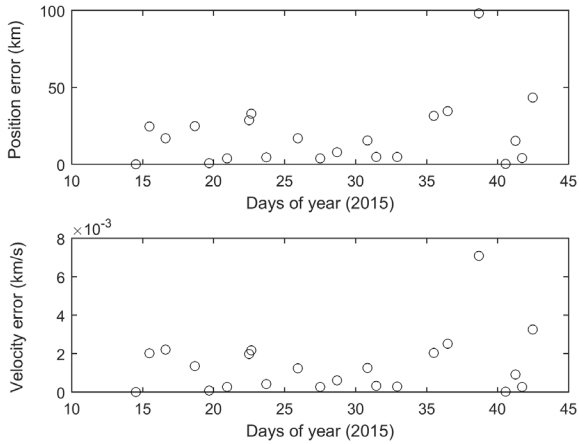


Fig. 13. Overlap analysis for TLE of COMS by propagation. TLE, two-line elements; COMS, Communication, Ocean and Meteorological Satellite.

analysis, and it is thus confirmed that TLE has several kilometers of position accuracy.

4.2 COMS Orbit Determination using OWL-Net Data

The orbit solutions were obtained under the conditions listed in Table 3, by using the OWL-Net data of two different arc lengths: 2 and 7 hours. The epoch time was set as the first observation time, and the a priori state vector was obtained by propagating TLE from the TLE epoch to the observation epoch, i.e., about 11 hours and 30 minutes. Note that the irregular data in Fig. 14 were excluded from the OD by a 3-sigma editor.

Fig. 15 shows the post-fit residuals of zero-mean with standard deviations of 2.8 arcseconds for RA and 1.4 arcseconds for DEC in both arc cases. These residuals are consistent with the known quality of OWL-Net observations

of a few arcseconds (Choi et al. 2018), which indicates that the estimated state is well converged to the true state. It verifies both the quality of the OWL-Net data and the applicability of the developed software to the actual system. According to the numerical simulations in Section 3.4, the positional accuracy of the orbit solution is expected to be about 1 km using such quality of optical data.

Table 4 addresses the Cartesian differences of the OD results with respect to TLE in topocentric radial-transverse-normal (RTN) coordinates. The positional differences are about 16.97 km with the short arc and 1.38 km with the long arc, and the differences in velocity are 1.13 m/s with the short arc and 0.17 m/s with the long arc. The differences are smaller for longer arc length, which is consistent with the previous analysis in Section 3.1. Moreover, the largest portion of the positional difference is in the radial direction, which reflects the characteristics of the optical system that only measures the projected angle of the celestial sphere. In both cases, the OD accuracy is reasonable considering the TLE accuracy of several tens of kilometers, and the accuracy is also consistent with a previous study of the OD for COMS using OWL-Net data (Choi et al. 2015).

Table 5 presents the differences between the OD results and TLE in the form of the orbital elements. The differences in the semi-major axis, eccentricity, and inclination decrease considerably as the arc length increases: the relative errors vary from 0.1% to 0.004% for the semi-major axis, more than 800% to 30% for the eccentricity, and from 27% to 0.2% for the inclination. The true longitude, which is typically applied in equatorial and circular orbits, however, had a relative error of under 0.01% in both cases. This can be explained by the fact that the velocity accuracy improves as the arc length increases, so the elements which depend

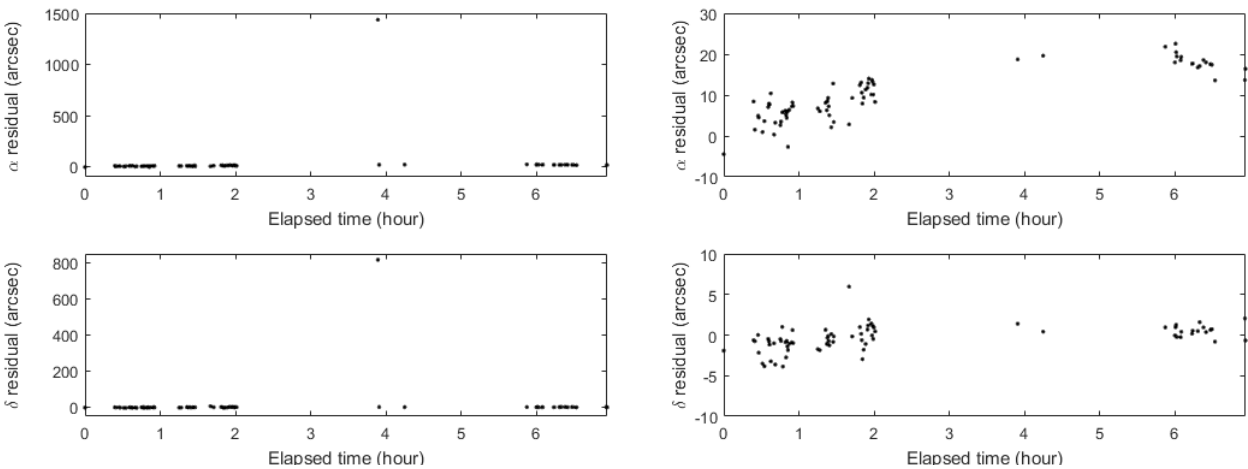


Fig. 14. Measurement residuals evaluated by two-line elements (left: whole data, right: except irregular data).

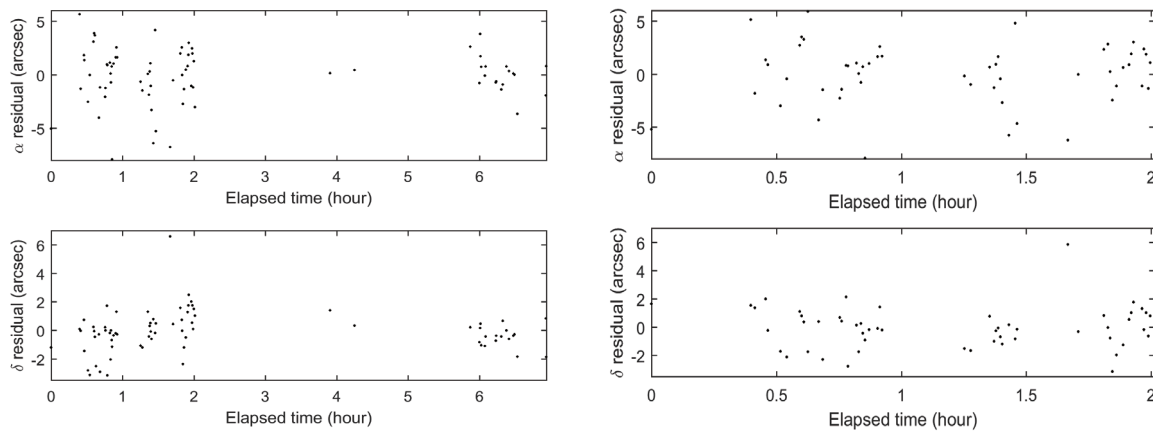


Fig. 15. Post-fit residuals of Communication, Ocean and Meteorological Satellite (left: 2-hour arc, right: 7-hour arc).

Table 4. Comparison of OD results to TLE in the form of topocentric RTN coordinates

	R (km)	T (km)	N (km)	V _R (km/s)	V _T (km/s)	V _N (km/s)
TLE	41,950.7629	-83.7702	4,264.6819	0.0064	3.0745	0.0003
2 hours OD	41,933.8004	-83.5815	4,264.0300	0.0071	3.0736	0.0005
(difference)	(-16.9625)	(0.1886)	(-65.19)	(0.0007)	(-0.0009)	(0.0002)
7 hours OD	41,949.3942	-83.6076	4,264.5496	0.0063	3.0747	0.0003
(difference)	(-1.3687)	(0.1626)	(-0.1323)	(-0.0001)	(0.0002)	(0.0000)

OD, orbit determination; TLE, two-line elements; RTN, radial-transverse-normal.

Table 5. Comparison of OD results to TLE in the form of Keplerian elements

	SMA (km)	ECC (°)	INC (°)	AOP (°)	RAAN (°)	MA (°)
TLE	42,164.66399	0.00012	0.00741	59.91997	224.06495	126.49676
2 hours OD	42,107.45527	0.00108	0.00944	56.81631	191.35710	162.28080
(difference)	(-57.20872)	(0.00096)	(0.00203)	(-3.10366)	(-32.70786)	(35.78404)
7 hours OD	42,166.43710	0.00008	0.00743	59.89850	264.93024	85.65472
(difference)	(1.77310)	(-0.00004)	(0.00001)	(-0.02147)	(40.86529)	(-40.84203)

OD, orbit determination; TLE, two-line elements; SMA, semi-major axis; ECC, eccentricity; INC, inclination; AOP, argument of perigee; RAAN, right ascension of the ascending node; MA, mean anomaly.

strongly on the velocity are considerably corrected.

Both orbit solutions were propagated for 24 hours and compared to TLE to evaluate the orbit prediction accuracy after a day. Fig. 16 shows the differences in position and velocity in topocentric RTN coordinates. The prediction accuracy of the long arc solution was 20 times better than that of the short arc solution; the positional differences were hundreds of kilometers in the short arc cases and about 20 km in the long arc case for a day. Considering the field of view of OWL-Net, which is 1.75 degrees (Park et al. 2013), it is confirmed that OWL-Net data with an arc length longer than 2 hours can provide accurate orbit solutions to continue monitoring GEO satellites for a day.

5. CONCLUSIONS

In this study, we have developed and verified a batch least

square estimator which utilizes optical observation data to determine the orbits of GEO objects. The characteristics of the observation error sources and OD results were analyzed by numerical simulations using pseudo-optical observation data. Furthermore, the developed batch filter was applied to OD for a GEO satellite, COMS, using real observation data from OWL-Net and the results were compared with TLE.

The OD property analysis using pseudo-observation data was carried out in terms of arc length (number of observation data points), observation intervals, a priori uncertainty, measurement noise, and clock errors. The analytic results verified that the accuracy of the OD improves as the arc length is increased and the observation interval is shortened and that it is more efficient to adjust the arc length to get a more precise orbit solution. Also, it was confirmed that the a priori covariance prevents the scatter of the OD results for a GEO satellite from the a priori guess, even with low measurement quality. Regarding

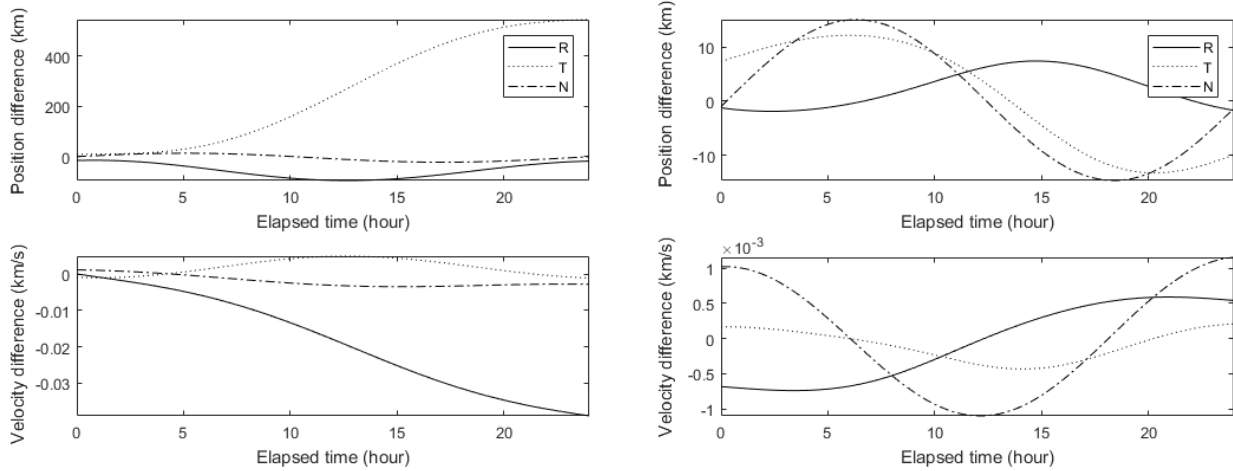


Fig. 16. Position and velocity differences of OD results for COMS compared to TLE for 24 hours in topocentric RTN coordinates (left: 2-hour solution, right: 7-hour solution). OD, orbit determination; COMS, Communication, Ocean and Meteorological Satellite; TLE, two-line elements; RTN, radial-transverse-normal.

observation noise, the error in the OD was proportional to the level of noise and the derived values were consistent with the geometric estimation. In the case of clock offset, the positional error was consistent with the orbital motion of the space object, and significant error occurred in case of clock mismatch.

The OD for COMS was performed using practical observation data of 2-hour and 7-hour-long arcs from OWL-Net. The observation residuals converged to a few arcseconds, which is close to the known value of the observation quality of OWL-Net. The OD accuracy was evaluated by comparison to TLE, which has an accuracy of several tens of kilometers, and the OD accuracy was found to be about 15 km and 1 km in the short and long arc cases, respectively.

Through this study, it was confirmed that appropriate observation weights based on the quality of observation data and an a priori covariance matrix based on the reliability of a priori states are important for obtaining more precise orbit solutions. The clock error which can be involved in the practical observation data from OWL-Net must be corrected. It was proven that the OWL-Net system can provide tracking data with reasonable quality, and continuous monitoring of GEO satellites is possible with the system. In addition, the precise dynamic model necessary to alternate GMAT is being developed and the system will be independently operated in the future.

ACKNOWLEDGMENTS

This research was supported by the development of

Electro-optical Space Surveillance System and through the Korea Astronomy and Space Science Institute funded by the National Research Council of Science and Technology, and by the Korea Astronomy and Space Science Institute under the R&D program (Project No. 2019-1-854-02) supervised by the Ministry of Science and ICT.

REFERENCES

Choi J, Jo JH, Roh KM, Son JY, Kim MJ, et al., Analysis of the angle-only orbit determination for optical tracking strategy of Korea GEO satellite, COMS, *Adv. Space Res.* 56, 1056-1066 (2015). <https://doi.org/10.1016/j.asr.2015.06.005>

Choi J, Jo JH, Yim HS, Choi EJ, Cho S, et al., Optical tracking data validation and orbit estimation for sparse observations of satellites by the OWL-Net, *Sensors*, 18, E1868 (2018). <https://doi.org/10.3390/s18061868>

Crassidis JL, Junkins JL, *Optimal Estimation of Dynamic Systems*, 2nd ed. (CRC press, New York, 2011).

Hughes SP, Qureshi RH, Cooley DS, Parker JJK, Verification and validation of the general mission analysis tool (GMAT). In *AIAA/AAS Astrodynamics Specialist Conference*, San Diego, CA, 4-7 Aug 2014. <https://doi.org/10.2514/6.2014-4151>

Lee E, Park SY, Shin B, Cho S, Choi EJ, et al., Orbit determination of KOMPSAT-1 and Cryosat-2 satellites using optical wide-field patrol network (OWL-Net) data with batch least squares filter, *J. Astron. Space Sci.* 34, 19-30 (2017). <https://doi.org/10.5140/JASS.2017.34.1.19>

Linares R, Jah MK, Crassidis JL, Nebelecky CK, Space object shape characterization and tracking using light curve and angles data, *J. Guid. Control. Dyn.* 37, 13-25 (2013). <https://doi.org/10.2514/6.2013-1151>

doi.org/10.2514/1.62986

Long AC, Cappellari JO Jr, Velez CE, Fuchs AJ, Goddard trajectory determination system (GTDS): mathematical theory (revision 1), National Aeronautics and Space Administration/Goddard Space Flight Center, FDD/552-89/001 and CSC/TR-89/6001 (1989).

Park JH, Yim HS, Choi YJ, Jo JH, Moon HK, et al., OWL-Net: A global network of robotic telescopes for satellite observation, *Adv. Space Res.* 62, 152-163 (2018). <https://doi.org/10.1016/j.asr.2018.04.008>

Park SY, Keum KH, Lee SW, Jin H, Park YS, et al., Development of a data reduction algorithm for optical wide field patrol, *J. Astron. Space Sci.* 30, 193-206 (2013). <https://doi.org/10.5140/JASS.2013.30.3.193>

Schutz B, Tapley B, Born GH, *Statistical Orbit Determination* (Amsterdam, Academic Press, 2004).

Son JY, Optical orbit determination of an active geosynchronous earth orbit satellite and tracking of low earth orbit satellite's re-entry, Master Thesis, University of Science and Technology (2015).

Tombasco J, Orbit estimation of geosynchronous objects via ground-based and space-based optical tracking, PhD Dissertation, University of Colorado (2011).

Vallado DA, Agapov V, Orbit determination results from optical measurements, In *AIAA/AAS Astrodynamics Specialist Conference*, Toronto, ON, 2-5 Aug 2010. <https://doi.org/10.2514/6.2010-7525>